Received: 25 October 2017 | Accepted: 5 January 2018
DOI: 10.1002/jcp.26424

ORIGINAL RESEARCH ARTICLE

WILEY Journal of Cellular Physiology

Long non-coding RNA TCONS_00041960 enhances osteogenesis and inhibits adipogenesis of rat bone marrow mesenchymal stem cell by targeting miR-204-5p and miR-125a-3p

Guowei Shang[1] | Yadong Wang[2] | Yan Xu[2] | Shanfeng Zhang[2] | Xiaoya Sun[2] | Hongya Guan[2] | Xuefeng Zhao[2] | Yisheng Wang[1] | Yuebai Li[2] | Guoqiang Zhao[3]

[1] Department of Orthopaedic Surgery, The First Affiliated Hospital of Zhengzhou University, Zhengzhou, China

[2] Department of Biochemistry and Molecular Biology, School of Basic Medical Sciences, Zhengzhou University, Zhengzhou, China

[3] Department of Microbiology and Immunology, School of Basic Medical Sciences, Zhengzhou University, Zhengzhou, China

Correspondence
Yisheng Wang, Department of Orthopaedic Surgery, The First Affiliated Hospital of Zhengzhou University, No.1 Jianshe East Road, Zhengzhou 450052, China.
Email: wangyisheng@zzu.edu.cn
Yuebai Li, Department of Biochemistry and Molecular Biology, School of Basic Medical Sciences, Zhengzhou University, No.100 Kexue Road, Zhengzhou 450001, China.
Email: liyuebai@zzu.edu.cn

Funding information
National Natural Science Foundation of China, Grant number: 81772427

A growing number of long non-coding RNAs (lncRNAs) have been found to be involved in diverse biological processes such as cell cycle regulation, embryonic development, and cell differentiation. However, limited knowledge is available concerning the underlying mechanisms of lncRNA functions. In this study, we found down-regulation of TCONS_00041960 during adipogenic and osteogenic differentiation of glucocorticoid-treated bone marrow mesenchymal stem cells (BMSCs). Furthermore, up-regulation of TCONS_00041960 promoted expression of osteogenic genes Runx2, osterix, and osteocalcin, and anti-adipogenic gene glucocorticoid-induced leucine zipper (GILZ). Conversely, expression of adipocyte-specific markers was decreased in the presence of over-expressed TCONS_00041960. Mechanistically, we determined that TCONS_00041960 as a competing endogenous RNA interacted with miR-204-5p and miR-125a-3p to regulate Runx2 and GILZ, respectively. Overall, we identified a new TCONS_00041960-miR-204-5p/miR-125a-3p-Runx2/GILZ axis involved in regulation of adipogenic and osteogenic differentiation of glucocorticoid-treated BMSCs.

KEYWORDS
bone marrow mesenchymal stem cells, differentiation, LncRNA TCONS_00041960, miR-125a-3p, miR-204-5p

1 | INTRODUCTION

Osteonecrosis of the femoral head (ONFH), also known as aseptic or ischemic necrosis of the femoral head, is a debilitating disease with ultimately head collapse and joint destruction. A recent study reported that the incidence rate of ONFH in Japan is 1.91 per 100,000 (Ikeuchi et al., 2015). In China, there are an estimated 8.12 million people aged 15 years and over suffering from ONFH (Zhao et al., 2015). Although the precise pathogenesis of ONFH remains unknown, the generally accepted theory is that traumatic or

non-traumatic injuries lead to the death of all cellular elements of bone (Mont & Hungerford, 1995). Extensive clinical use of glucocorticoids has been identified as the main risk factor for non-traumatic ONFH (Mont, Jones, & Hungerford, 2006; Zhao, Guo, & Li, 2013). Glucocorticoids can adversely affect the metabolism of osteoblasts, osteoclasts, and osteocytes, and enhance mesenchymal stem cell (MSC) differentiation into adipocytes, resulting in elevated intraosseous pressure, fat embolism, hypercoagulability that reduces blood supply to the femoral head, and finally ONFH (Drescher, Schlieper, Floege, & Eitner, 2011; Jones, 1993; Tan, Kang, & Pei, 2012; Weinstein, 2012).

Long non-coding RNAs (lncRNAs) are a relatively well-characterized class of non-coding RNA molecules of more than 200 nucleotides in length (Brosnan & Voinnet, 2009). LncRNAs play pivotal roles as regulatory molecules in a variety of biological processes such as cell cycle regulation, embryonic development, and cell differentiation (Fatica & Bozzoni, 2014; Kitagawa, Kitagawa, Kotake, Niida, & Ohhata, 2013; Zhang, Huang, Luo, & Li, 2014). A recent study demonstrated that lncRNAs interact with microRNAs (miRNAs) as competing endogenous RNAs (ceRNAs) to participate in the regulation of MSC differentiation and metabolism (Tye et al., 2015). LncRNA YAM-1 inhibits myoblast differentiation via regulation of miR-715 (Lu et al., 2013). LncRNA MEG3 may be involved in adipogenic and osteogenic differentiation of human adipose-derived stem cells (ADSCs) via miR-140-5p, which also inhibits osteogenic differentiation of bone marrow mesenchymal stem cells (BMSCs) from patients with postmenopausal osteoporosis by targeting miR-133a-3p (Li et al., 2017; Wang et al., 2017). Moreover, miRNAs are involved in multiple biological processes by regulating their mRNA targets (Ambros & Chen, 2007; Pasquinelli, 2012). Therefore, we hypothesized that a lncRNA-miRNA-mRNA axis might play an important role in regulating differentiation of MSCs.

Although an increasing number of lncRNAs have been found to be involved in regulation of various types of MSC differentiation, the functions of lncRNAs during ONFH have not been elucidated yet. In our study, we investigated lncRNA TCONS_00041960 in glucocorticoid-treated BMSCs by lncRNA microarray analysis. Further bioinformatics analysis and functional assays indicated that TCONS_00041960 interacted with miR-204-5p and miR-125a-3p to regulate adipogenic and osteogenic differentiation of BMSCs. Therefore, we sought to reveal a new TCONS_00041960-miRNA-mRNA axis that regulates adipogenic and osteogenic differentiation of glucocorticoid-treated BMSCs.

2 | MATERIALS AND METHODS

2.1 | Isolation and establishment of BMSCs

Six Sprague–Dawley (SD) rats weighing 180–220 g were purchased from the Henan Experimental Animals Center (Zhengzhou, China). BMSCs were isolated from their tibias and fibulas. Bone marrow was washed in a cell culture dish with low glucose Dulbecco's modified Eagle's medium (Biological Industries, Cromwell, CT) containing 15% fetal bovine serum (Biological Industries), 100 U/ml penicillin, 100 μg/ml streptomycin, and 20 mmol/L Hepes. Cells were seeded at a density of 6×10^6 cells/ml and cultured at 37 °C in a humidified atmosphere with 5% CO_2. The growth and morphology of passage (P) 3 cells as well as surface markers CD29, CD34, CD45, and CD105 were analyzed using a FACScan flow cytometer (BD Biosciences, San Jose, CA). The Animal Experimentation Ethics Committee of Zhengzhou University has approved all procedures in this study.

2.2 | Steroid treatment

P3 or 4 BMSCs were treated with 1×10^{-6} mol/L dexamethasone (Sigma–Aldrich, St. Louis, MO). The medium was replaced every 2 days. Cell morphology and the appearance of cytoplasmic lipid droplets were observed and recorded under a phase contrast microscope.

2.3 | LncRNA microarray analysis

BMSCs were treated with 1×10^{-6} mol/L dexamethasone for 7 days, the medium was removed, and TRIZOL Reagent (Invitrogen, Carlsbad, CA) was added at 1 ml per cm^2 of the culture vessel, followed by snap freezing in liquid nitrogen and shipment on dry ice to OEBiotech Co., Ltd. (Shanghai, China). An Agilent Rat lncRNA Microarray V2 (8*60 K, Design ID: 062716) was used for analysis.

2.4 | Cell transfection

Recombinant lentiviruses carrying TCONS_00041960 (Ex-lnc), small interfering RNA (siRNA) against TCONS_00041960 (si-lnc), or negative control oligonucleotides (Ex-NC or si-NC) were purchased from Shanghai GenePharma Co., Ltd. (Shanghai, China). For viral infections, BMSCs were cultured overnight and then infected with lentiviruses (multiplicity of infection = 2) in the presence of 5 μg/ml polybrene (Sigma–Aldrich). At 8 hr post-infection, the medium was replaced with fresh complete medium. The infected cells were selected with 1 μg/ml puromycin for 7 days.

For transfections, miR-204-5p mimic or inhibitor, miR-125a-3p mimic or inhibitor, and scrambled oligonucleotides (miR-NC) were purchased from Shanghai GenePharma Co., Ltd. BMSCs were transfected in 6-well plates at 60% confluence using Lipofectamine™ 2000 (Invitrogen), according to the manufacturer's instructions.

2.5 | RNA extraction and quantitative reverse transcription-polymerase chain reaction (qRT-PCR)

Total RNA (including lncRNAs and mRNAs) was extracted using a total RNA extraction kit (Omega, Norcross, GA), according to the manufacturer's instructions. The RNA quality and concentration were assessed with a NanoDrop 1000 Spectrophotometer (Thermo Fisher Scientific, Waltham, MA). cDNA was synthesized using a RevertAid First Strand cDNA kit (Thermo Fisher Scientific). SYBR Green I (TaKaRa, Dalian, China) was used for qRT-PCR with

glyceraldehyde-3-phosphate dehydrogenase (GAPDH) as an endogenous control. To analyze the expression of miR-204-5p and miR-125a-3p, miRNAs were extracted using an miRcute miRNA isolation kit (Tiangen Biotech, Beijing, China). Quantitative PCR was carried out using miR-204-5p or miR-125a-3p Hairpin-it™ miRNA qRT-PCR Kits (GenePharma Co., Ltd) with U6 as an internal reference. The results were assessed by the $2^{-\Delta\Delta Ct}$ method. All experiments were performed in triplicate using an ABI 7500 fast cycler.

2.6 | Western blotting

Total proteins were extracted using RIPA buffer containing PMSF, and protein concentrations were measured using BCA protein assay kit (Beyotime, Haimen, China), according to the manufacturer's protocol. SDS-PAGE was performed to separate equal amounts of proteins that were then transferred to a PVDF membranes (Invitrogen), followed by blocking with 5% bovine serum albumin (BSA). Primary antibodies, anti-runt-related transcription factor 2 (Runx2) (1:500, Abcam, Cambridge, MA), anti-osterix (1:500, Abcam), anti-osteocalcin (1:300, Santa Cruz Biotechnology, Dallas, TX), anti-PPARγ (1:1,000, Abcam), anti-C/EBPα (1:500, Santa Cruz Biotechnology), and anti-glucocorticoid-induced leucine zipper (GILZ) (1:500, Santa Cruz Biotechnology), were applied overnight at 4 °C. Goat anti-rabbit IgG (H + L) horseradish peroxidase (HRP) (1:5,000; Sungene Biotech, Tianjing, China) as the secondary antibody was applied at room temperature for 1 hr. Detection was performed using a chemiluminescence (ECL) detection kit (Amersham Pharmacia Biotech, Piscataway, NJ). GAPDH (Santa Cruz Biotechnology) was used as an internal control for normalization.

2.7 | Luciferase reporter assay

Bioinformatics analysis predicted that TCONS_00041960 might interact with miR-204-5p or miR-125a-3p. Moreover, Runx2 and GILZ are potential target genes of miR-204-5p, and miR-125a-3p, respectively. We constructed recombinant plasmids pmirGLO-TCONS_00041960-wt/pmirGLO-TCONS_00041960-mut, pmirGLO-Runx2-wt/pmirGLO-Runx2-mut, and pmirGLO-GILZ-wt/pmirGLO-GILZ-mut. HEK293T cells (HANBIO, Shanghai, China) were co-transfected with miRNAs (miR-204-5p mimics, miR-125a-3p mimics, or miR-NC) and recombinant plasmids using Lipofectamine™ 2000. Luciferase activity was determined using a Dual Luciferase Reporter Assay System (Promega, Madison, WI), according to the manufacturer's instructions.

2.8 | RNA immunoprecipitation (RIP) assay

The RIP assay was performed using an EZ-Magna RIP RNA-binding protein immunoprecipitation kit (Millipor), following the manufacturer's protocol. BMSCs were lysed in RNA lysis buffer containing protease and RNase inhibitors. The protein extract was incubated with RIP wash buffer containing magnetic beads conjugated with a human anti-argonaute 2 (Ago2) antibody (Millipore) or mouse IgG (Millipore) as a negative control for 2 hr at 4 °C. Unbound proteins were digested with proteinase K, and co-immunoprecipitated RNA was isolated. Then, qRT-PCR analysis was performed to determine the presence of binding targets.

2.9 | Surface plasmon resonance (SPR) assay

The SPR assay was performed with HBS-EP buffer (10 mM HEPES, 150 mM NaCl, 3.4 mM EDTA, and 0.005% P20, pH 7.4) on a BiacoreT200 (BIAcore AB, GE Healthcare) using a carboxy methylated dextran-coated sensor chip at 25 °C. Before immobilization, neutravidin, 0.2M N-ethyl-N′-[3-(diethylamino)propyl] carbodiimide, and 50 mM N-hydroxysuccinimide were mixed at 1:1:1 to activate surfaces. The surfaces were then blocked with 0.5 M ethanolamine-HCl (pH 8.5) for 7 min. Biotin-labeled single-stranded RNA-harboring wild-type TCONS_00041960 or mutant TCONS_00041960 were captured on sensor chip surfaces. The other two empty channels served as a reference. miR-204-5p, miR-125a-3p, or scrambled oligonucleotides at various concentrations (31.25, 62.5, 125, 250, and 500 nM) were injected at 10 µl/min across all surfaces for 2 min and then allowed to dissociate for 15 min. The resu lts were recorded and processed in the BIA evaluation system.

2.10 | Oil red O staining

BMSCs were fixed in 10% formalin for 30 min at room temperature, washed with sterile water, and then incubated with 60% isopropanol for 5 min. The cells were stained with filtered oil red O (Sigma) for 10 min at room temperature. Cell morphology and staining were observed under a microscope.

2.11 | Determination of cellular triglyceride (TG) contents

A Triglyceride Determination Kit (Applygen, Beijing, China) was used to detect cellular TG contents. BMSCs were collected and centrifuged at 1,000 rpm for 10 min, washed twice with PBS, and lysed with 1% Triton X-100 for 30 min. Then, a mixture of 3 µl cytochylema and 300 µl of working solution was added to each well of a 96-well plate including blank and calibration wells. Absorbances were determined at a wavelength of 500 nm after incubation at 37 °C for 5 min.

2.12 | Alkaline phosphatase (ALP) activity assay

The ALP activity assay was performed using an enzyme-linked immunosorbent assay test kit (R&D Systems, Minneapolis, MN). BMSCs were collected in buffer solution and centrifuged at 15,000 rpm for 15 min at 4 °C. The supernatant was diluted fivefold by adding dilute solution to sample wells, followed by incubation at 37 °C for 30 min. Plates were washed with water, and HRP was added to the sample wells, followed by incubation at 37 °C for 30 min. After washing with water again, Chromogenic solution was added, followed

by incubation at 37 °C for 15 min. Finally, termination solution was added and absorbances were measured at a wavelength of 450 nm.

2.13 | Statistics

SPSS17.0 software was used for all statistical analyses. All results are expressed as the mean ± standard deviation. Student's *t*-test and one-way analysis of variance were used for comparisons of means. A value of $p < 0.05$ was considered to be statistically significant.

3 | RESULTS

3.1 | TCONS_00041960 expression down-regulates in glucocorticoid-treated BMSCs

To identify lncRNA expression during adipogenic differentiation of rat BMSCs, we performed microarray analysis of BMSCs treated with glucocorticoid for 7 days. Adipocyte differentiation was confirmed by oil red O staining (Figure 1a). The lncRNA microarray analysis identified 151 differentially expressed lncRNAs of which 79 were up-regulated and 72 were down-regulated in the Model group compared with the Blank group. We chose lncRNAs with at least a threefold change in expression as displayed in a heat map (Figure 1b). To confirm the microarray results, we randomly selected four differentially expressed lncRNAs (TCONS_00041960, XR_085692.2, TCONS_00036420, and TCONS_00083120) to verify their expression by qRT-PCR. The results showed that the expression of these lncRNAs was consistent with the microarray results (Figure 1c–f). We choose lncRNA TCONS_00041960 for further experiments.

3.2 | TCONS_00041960 up-regulation promotes osteogenic differentiation and attenuates adipogenic differentiation of glucocorticoid-treated rat BMSCs

To investigate the functional roles of TCONS_00041960 in adipogenesis and osteogenesis, cells were divided into four groups: Blank group, untransfected and untreated BMSCs; Dex group, 1×10^{-6} mol/L dexamethasone-treated BMSCs; Ex-NC group, Ex-NC-transfected and 1×10^{-6} mol/L dexamethasone-treated BMSCs; Ex-Lnc group, Ex-lnc-transfected and 1×10^{-6} mol/L dexamethasone-treated BMSCs. Next, we detected TCONS_00041960 expression after 72 hr. qRT-PCR revealed that TCONS_00041960 expression was higher in the Ex-Lnc group compared with the Dex group, which confirmed successful transfection (Figure 2a). Furthermore, the qRT-PCR data indicated that expression of osteogenic differentiation-related marker genes Runx2, osterix, and osteocalcin was significantly increased in the Ex-Lnc group compared with Dex and Ex-NC groups. Adipogenic differentiation-related marker genes PPARγ, C/EBPα, and GILZ had obvious differential expression. GILZ expression was decreased, but PPARγ and C/EBPα expression was up-regulated significantly (Figure 2b). Western blotting results were consistent with the qRT-PCR data (Figure 2c). Next, we performed oil red O staining to verify lipid droplets in BMSCs during adipogenesis. On day 14 of glucocorticoid treatment, oil red O staining showed that the Dex group had more lipid accumulation than the Blank group, but the Ex-Lnc group had decreased lipid droplet formation compared with the Dex group (Figure 2f). To confirm the staining pattern, we measured TG content in the Ex-Lnc group, which was lower than that in the Dex group at day 14

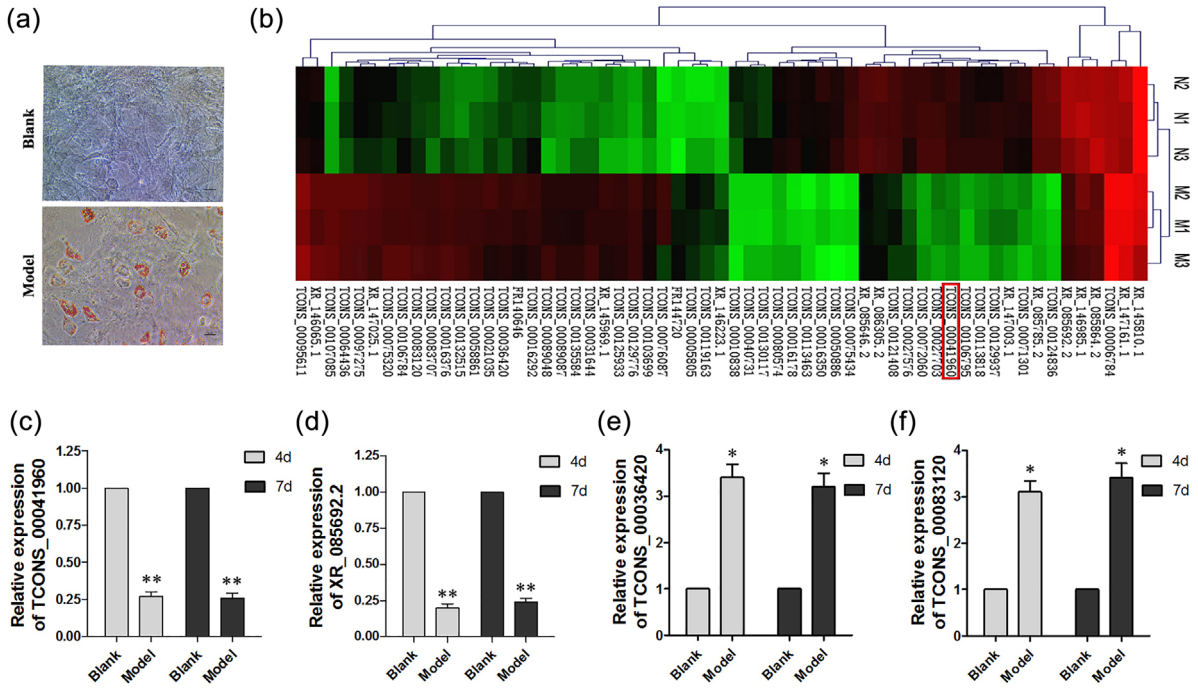

FIGURE 1 Expression of TCONS_00041960 during adipogenesis of BMSCs. (a) Oil red O staining to detect lipid accumulation under light microscopy. Magnification, ×200. (b) Heat map of lncRNAs differentially expressed in the Model group compared with the Blank group. (c–f) Microarray results of four differentially expressed lncRNAs (TCONS_00041960, XR_085692.2, TCONS_00036420, and TCONS_00083120) were confirmed by qRT-PCR. $^{*}p < 0.05$, $^{**}p < 0.01$ versus Blank group

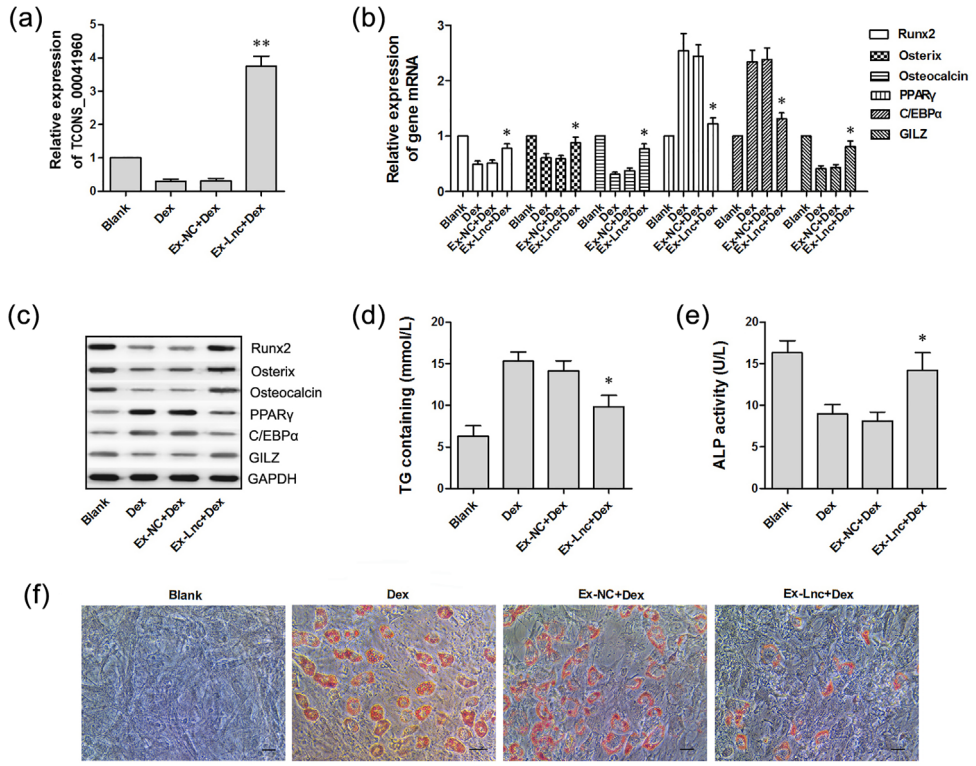

FIGURE 2 Functional roles of TCONS_00041960 in adipogenesis and osteogenesis. (a) BMSCs were transfected with Ex-lnc or Ex-NC and analyzed by qRT-PCR. GAPDH served as an internal control. (b) Osteogenesis-associated genes (Runx2, osterix, and osteocalcin) and adipogenesis-associated genes (PPARγ, C/EBPα, and GILZ) were detected by qRT-PCR. Data were normalized to GAPDH mRNA levels. (c) Western blot analysis to verify osteogenesis-associated (Runx2, osterix, and osteocalcin) and adipogenesisassociated (PPARγ, C/EBPα, and GILZ) protein levels. GAPDH was used as a reference. (d and e) TG contents and ALP activity were measured at day 14. (f) Oil red O staining was performed at day 14. $^{*}p < 0.05$, $^{**}p < 0.01$ versus Dex or Ex-NC groups

(Figure 2d) Moreover, ALP activity in the Ex-Lnc group was higher than that in the Dex group at day 14 (Figure 2e). These results demonstrated that TCONS_00041960 up-regulation clearly promoted osteogenic differentiation and suppressed adipogenic differentiation of glucocorticoid-treated rat BMSCs.

3.3 | TCONS_00041960 interacts with miR-204-5p and miR-125a-3p

To elucidate the underlying molecular mechanism of the TCONS_00041960 interaction with miRNAs, we performed bioinformatics analysis (TargetScanand miRBase) to predict potential binding sites between TCONS_0004196 and miRNAs. We found that TCONS_00041960 contains sequences that recognize the seed regions of miR-204-5p and miR-125a-3p (Figure 3a). To confirm interactions between TCONS_00041960 and miR-204-5p or miR-125a-3p, we conducted luciferase assays. The sequences of wild-type or mutant-type TCONS_00041960 without miR-204-5p- or miR-125a-3p-binding sites were inserted downstream of the luciferase gene to construct the plasmid-TCONS_00041960 vector (Figure 3b). The results showed that the luciferase activity of the group co-transfected with wild-type TCONS_0041960 and miR-204-5p mimics in HEK 293T cells was significantly reduced compared with that of the other three groups (Figure 3c). Furthermore, the luciferase activity of the group co-transfected with wild-type TCONS_0041960 and miR-125a-3p mimics had clearly decreased luciferase activity compared with that of the other three groups (Figure 3d). These results indicated that specific sequences of miR-204-5p or miR-125a-3p can bind to the TCONS_0004196 sequence. To verify these results, we performed RIP assays. The subsequent qRT-PCR results showed that TCONS_0041960 and miR-204-5p or miR-12a-3p were preferentially enriched in Ago2-containing beads compared with control IgG immunoprecipitates, indicating that TCONS_0004196 bound to miR-204-5p and miR-125a-3p (Figure 3e). We then performed SPR assays that revealed positive binding between wild-type TCONS_0004196 and miR-204-5p mimics, but not between mutant TCONS_0004196 and miR-204-5p (Figure 3f). In addition, positive binding was observed in the group co-transfected with wild-type TCONS_0004196 and miR-125a-3p mimics compared with the other three groups (Figure 3g). Furthermore, we transfected rat BMSCs with miR-204-5p mimics or inhibitor, miR-125a-3p mimics or inhibitor, and mimic or inhibitor controls. qRT-PCR analysis showed that TCONS_0004196 expression was down-regulated in miR-204-5p and miR-125a-3p mimics groups and up-regulated in miR-204-5p and miR-125a-3p inhibitor groups compared with the negative control group (Figure 3h). These data revealed that miR-204-5p and miR-125a-3p regulated TCONS_0004196 expression. Next, we verified whether TCONS_0004196 affected miR-204-5p and miR-125a-3p

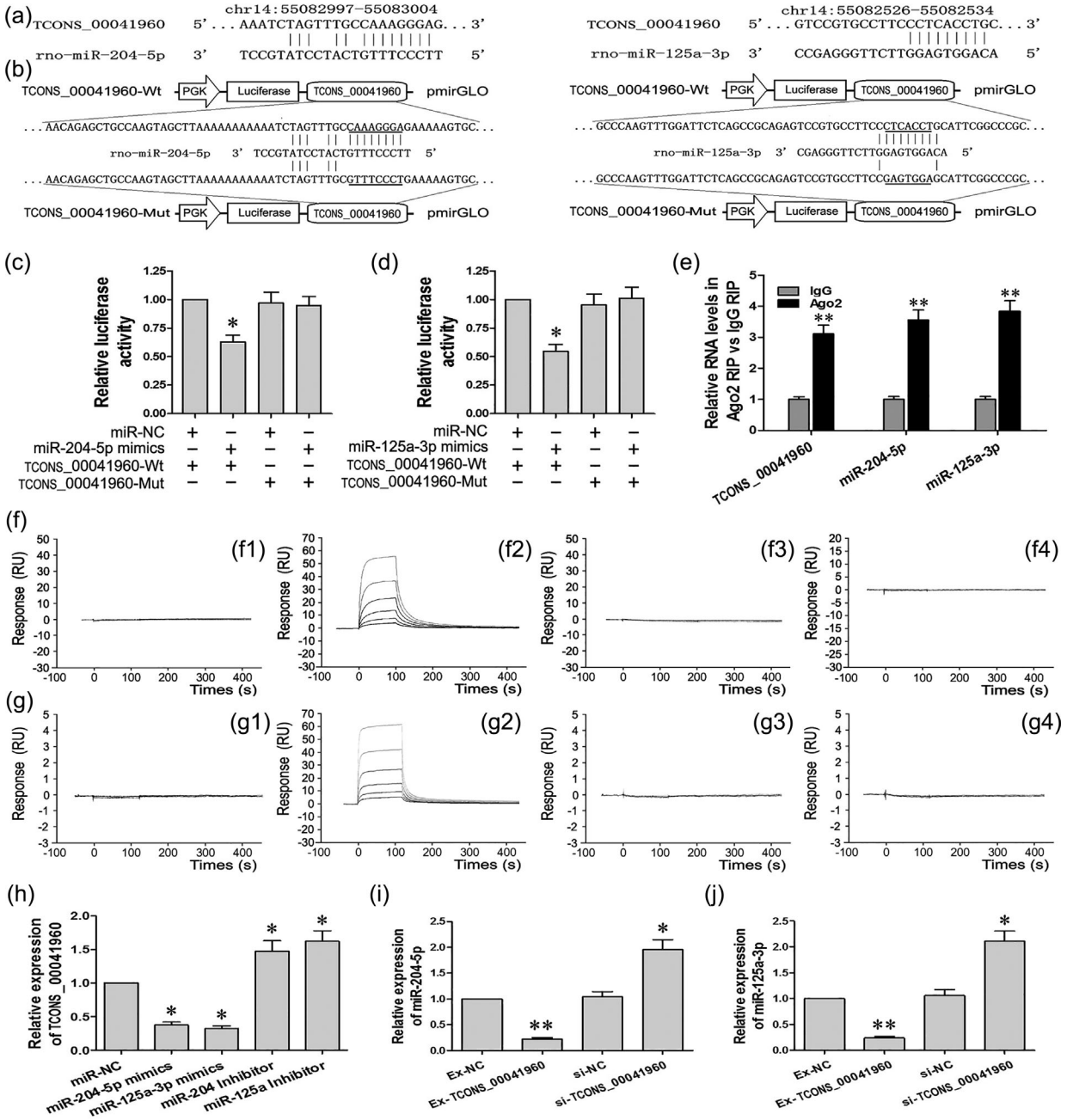

FIGURE 3 TCONS_0004196 interacts with miR-204-5p and miR-125a-3p. (a) Putative binding sites between TCONS_0004196 and miR-204-5p or miR-125a-3p. (b) Mutations were generated in TCONS_0004196-binding sites of miR-204-5p or miR-125a-3p. (c and d) Luciferase activities of wild-type or mutant-type TCONS_0004196 co-transfected with miR-204-5p or miR-125a-3p mimics. (e) Extracts of BMSCs were subjected to RIP assays with an anti-Ago2 antibody or IgG. (f) SPR assays were performed: hybridization on sensor chips between wild-type TCONS_0004196 and miR-204-5p negative control (f1), wild-type TCONS_0004196 and miR-204-5p mimics (f2), mutant TCONS_0004196 and miR-204-5p negative control (f3), and mutant TCONS_0004196 and miR-204-5p mimics (f4). (g) SPR assay were performed. Hybridization on sensor chips between wild-type TCONS_0004196 and miR-125a-3p negative control (g1), wild-type TCONS_0004196 and miR-125a-3p mimics (g2), mutant TCONS_0004196 and miR-125a-3p negative control (g3), and mutant TCONS_0004196 and miR-125a-3p mimics (g4). (h) TCONS_0004196 expression was regulated by miR-204-5p and miR-125a-3p mimics or inhibitors. GAPDH served as an internal control. (i and j) miR-204-5p and miR-125a-3p expression was regulated by Ex-TCONS_0004196 and si-TCONS_0004196. U6 served as an internal control. $^{*}p < 0.05$, $^{**}p < 0.01$

expression. We transfected rat BMSCs with recombinant lentivirus TCONS_0004196 (Ex-TCONS_0004196), siRNA lentivirus TCONS_0004196 (si-TCONS_0004196), or the relevant recombinant lentivirus negative controls (Ex-NC or si-NC). Ex-TCONS_0004196 suppressed miR-204-5p expression, but si-TCONS_0004196 elevated miR-204-5p expression. miR-125a-3p expression was down-regulated by Ex-TCONS_0004196 and up-regulated by si-TCONS_0004196 (Figures 3i and 3j). Taken together, these data showed that TCONS_0004196 interacted with miR-204-5p and miR-125a-3p.

3.4 | Runx2 and GILZ are direct targets of miR-204-5p and miR-125a-5p, respectively

Bioinformatics analysis (TargetScan and miRBase) showed that the recognition sequences of miR-204-5p and miR-125a-3p matched the 3′-untranslated region sequences of Runx2 and GILZ, respectively (Figures 4a and 4b), revealing that Runx2 is a potential target of miR-204-5p and GILZ is a candidate target of miR-125a-3p. To test these hypotheses, we transfected miR-204-5p mimics, miR-125a-3p mimics, or scramble oligonucleotides into rat BMSCs and then measured Runx2 and GILZ protein levels. Western blotting results showed that Runx2 and GILZ were down-regulated in miR-204-5p and miR-125a-3p mimics groups, respectively (Figures 4c and 4d). Next, pmirGLO-Runx2-wt or pmirGLO-Runx2-mut were co-transfected with miR-204-5p mimics or scrambled oligonucleotides, and pmirGLO-GILZ-wt or pmirGLO-GILZ-mut were co-transfected with miR-125a-3p mimics or scrambled oligonucleotides into HEK 293T cells. Then, luciferase activities were measured, which showed that miR-204-5p mimics reduced the luciferase activity of pmirGLO-Runx2-wt, but not that of pmirGLO-Runx2-mut. Furthermore, miR-125a-3p mimics deceased the luciferase activity of pmirGLO-GILZ-wt, but not that of pmirGLO-GILZ-mut (Figures 4e and 4f). These results demonstrated that miR-204-5p and miR-125a-5p directly targeted Runx2 and GILZ, respectively.

3.5 | Down-regulation of miR-204-5p or miR-125a-3p enhances osteogenesis and suppresses adipogenesis in glucocorticoid-treated rat BMSCs

We next examined the functional roles of miR-204-5p and miR-125a-3p during adipogenesis and osteogenesis of glucocorticoid-treated rat BMSCs. Dexamethasone-treated BMSCs were transfected with miR-204-5p inhibitor (miR-204-5p inhibitor group) or miR-125a-3p inhibitor (miR-125a-3p inhibitor group). qRT-PCR showed that miR-204-5p expression was significantly lower in the miR-204-5p inhibitor group than in the Dex group (Figure 5a). miR-125a-3p expression was also clearly suppressed in the miR-125a-3p inhibitor group compared with the Dex group (Figure 5b), which confirmed successful transfection. Based on these data, Runx2 and GILZ were direct targets of miR-204-5p and miR-125a-5p, respectively. We measured Runx2 and GILZ gene expression levels by qRT-PCR and found that Runx2 expression was up-regulated in the miR-204-5p inhibitor group compared with the Dex group, and GILZ expression was higher in the miR-125a-3p inhibitor group than in the Dex group (Figure 5c). Moreover, expression of osteogenesis-related marker genes, such as osterix and osteocalcin, was increased in the miR-204-5p inhibitor group compared with the Dex group. Expression of adipogenesis-related marker genes, such as PPARγ and C/EBPα, was decreased in the miR-125a-3p inhibitor group compared with the Dex group (Figure 5e). Western blot data were consistent with the qRT-PCR results (Figures 5d and 5f). We also detected TG contents and ALP activity in BMSCs on day 14. TG contents were decreased in the miR-125-3p inhibitor group compared with the Dex group (Figure 5g). ALP activity in the miR-204-5p inhibitor group was higher than in the Dex group (Figure 5h). Correspondingly, lipid droplet accumulation in the miR-125-3p inhibitor group was reduced (Figure 5i). Collectively, these data suggested that down-regulation of miR-204-5p and miR-125a-3p enhances osteogenesis and inhibits adipogenesis of glucocorticoid-treated rat BMSCs.

3.6 | Up-regulation of TCONS_0004196 enhances osteogenic differentiation and attenuates adipogenic differentiation of glucocorticoid-treated rat BMSCs by targeting miR-204-5p and miR-125a-3p

To confirm whether the effect of up-regulation TCONS_0004196 was consistent with down-regulation miR-204-5p or miR-125a-3p during osteogenesis and adipogenesis, we next transfected dexamethasone-

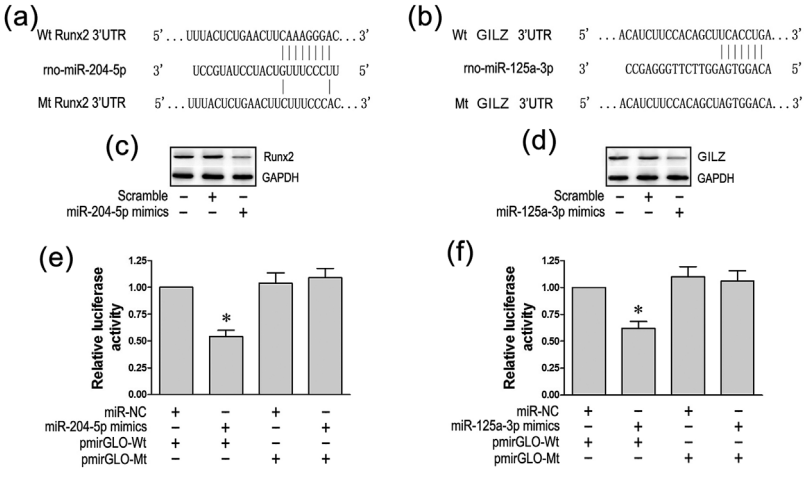

FIGURE 4 Runx2 and GILZ are direct targets of miR-204-5p and miR-125a-5p, respectively. (a and b) Putative binding sites between miR-204-5p and Runx2, and between miR-125a-5p and GILZ. (c and d) Western blot analysis of Runx2 and GILZ expression in transfected cells. GAPDH was used as an internal reference. (e and f) Dual luciferase assays were performed in cells co-transfected with wild-type or mutant pmirGLO-Runx2 and wild-type or mutant pmirGLO-GILZ with miR-204-5p and miR-125a-3p. *$p < 0.05$

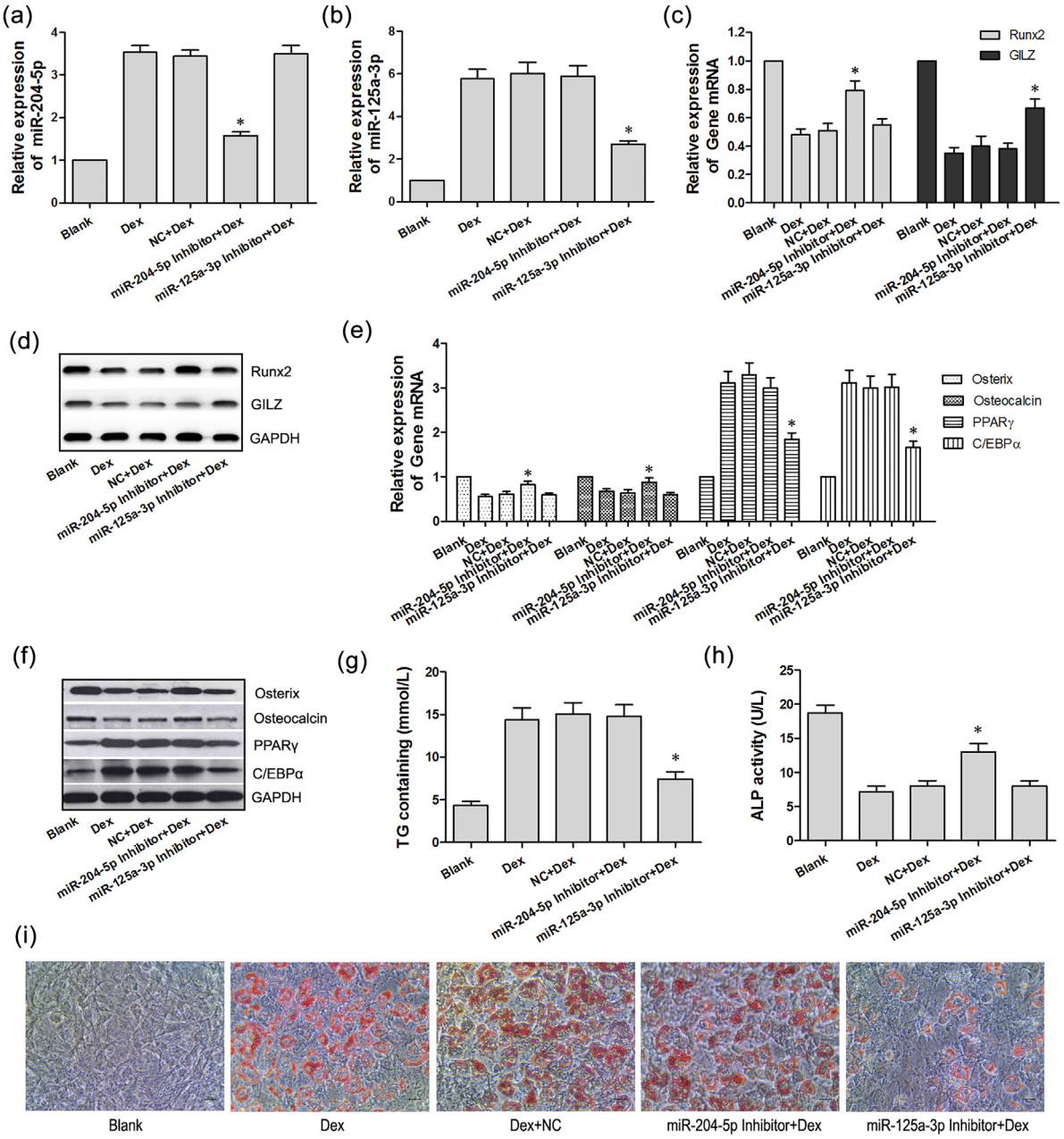

FIGURE 5 Down-regulation of miR-204-5p and miR-125a-3p enhances osteogenesis and suppresses adipogenesis of glucocorticoid-treated rat BMSCs. Blank group, non-transfected and untreated BMSCs; Dex group, dexamethasone-treated BMSCs; NC group, transfected with the negative control and treated with dexamethasone; miR-204-5p inhibitor group, transfected with miR-204-5p inhibitor and treated with dexamethasone; miR-125a-3p inhibitor group, transfected with miR-125a-3p inhibitor and treated with dexamethasone. (a and b) Dexamethasone-treated BMSCs transfected with miR-204-5p inhibitor or miR-125a-3p inhibitor were analyzed by qRT-PCR. U6 served as an internal control. (c–f) qRT-PCR analysis and western blotting were used to detect expression of osteogenesis-associated genes Runx2, osterix, and osteocalcin, and adipogenesis-associated genes PPARγ, C/EBPα, and GILZ. Data were normalized to GAPDH mRNA levels. (g and h) TG contents and ALP activity were measured at day 14. (i) Oil red O staining was performed at day 14. *$p < 0.05$

treated rat BMSCs with Ex-lnc, miR-204-5p mimics or inhibitor, and miR-125a-3p mimics or inhibitor. qRT-PCR analysis showed down-regulation of miR-204-5p expression in the miR-204-5p inhibitor group compared with the Dex group (Figure 6a), and reduced expression of miR-125a-3p in the miR-125a-3p inhibitor group compared with the Dex group (Figure 6b), which confirmed successful transfections. Accordingly, the qRT-PCR data showed that expression of osteogenic differentiation-related marker genes Runx2, osterix, and osteocalcin was significantly increased in Ex-Lnc and miR-204-5p inhibitor groups compared with the Dex group. Simultaneously, adipogenic differentiation-related marker genes PPARγ, C/EBPα, and GILZ were obviously expressed differentially. GILZ was up-regulated in Ex-Lnc and miR-125a-3p inhibitor groups, while PPARγ and C/EBPα were suppressed to a significant extent (Figure 6c). These

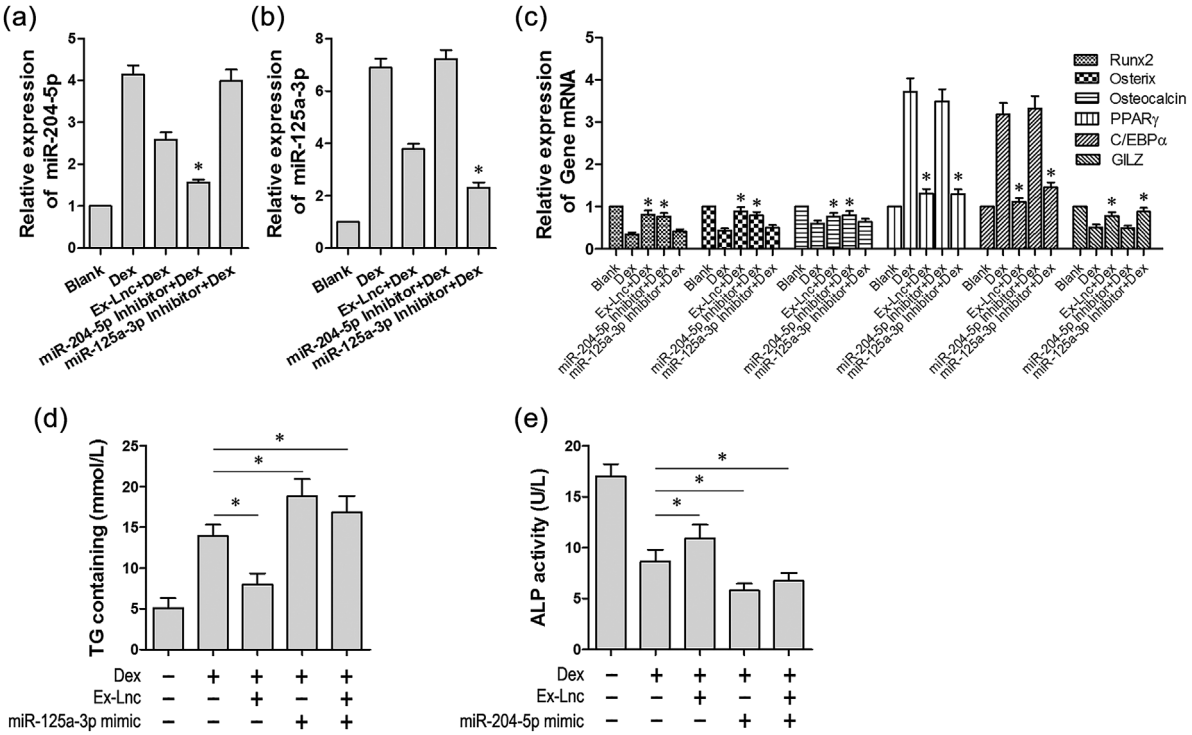

FIGURE 6 TCONS_0004196 regulates osteogenic and adipogenic differentiation of glucocorticoid-treated rat BMSCs by targeting miR-204-5p and miR-125a-3p. (a and b) BMSCs were transfected with recombinant lentiviruses carrying TCONS_00041960, miR-204-5p inhibitor, or miR-125a-3p inhibitor and then analyzed by qRT-PCR. U6 served as an internal control. (c) Expression of osteogenesis-associated genes (Runx2, osterix, and osteocalcin) and adipogenesis-associated genes (PPARγ, C/EBPα, and GILZ) was detected by qRT-PCR. Data were normalized to GAPDH mRNA levels. (d) TG contents were measured in rat BMSCs transfected with recombinant lentiviruses carrying TCONS_00041960 or miR-125a-3p mimics and cotransfected with recombinant lentiviruses carrying TCONS_00041960 and miR-125a-3p mimics. (e) ALP activity was detected in rat BMSCs transfected with recombinant lentiviruses carrying TCONS_00041960 or miR-204-5p mimics and co-transfected with recombinant lentiviruses carrying TCONS_00041960 and miR-204-5p mimics. *$p < 0.05$

data demonstrated that up-regulation of TCONS_0004196 had the same effect as down-regulation of miR-204-5p or miR-125a-3p. Moreover, TG contents were reduced in the Ex-Lnc group compared with the Dex group, but increased in the miR-125a-3p mimics group. In addition, TG contents were higher in the group co-transfected with Ex-Lnc and miR-125a-3p mimics (Figure 6d). Increased ALP activity was also observed in the Ex-Lnc group compared with the Dex group, but was reduced in the miR-204-5p mimics group. Furthermore, ALP activity was decreased in the group co-transfected with Ex-Lnc and miR-204-5p mimics (Figure 6e). Taken together, these data indicated that TCONS_0004196 up-regulation enhanced osteogenic differentiation and attenuated adipogenic differentiation of glucocorticoid-treated rat BMSCs by targeting miR-204-5p and miR-125a-3p.

4 | DISCUSSION

LncRNAs are a newly discovered class of regulatory RNAs involved in diverse biological processes of cells (Kung, Colognori, & Lee, 2013). Recent studies have demonstrated that many lncRNAs play important roles in regulating adipogenesis and osteogenesis of MSCs. For example, NEAT1, a nuclear lncRNA, promotes adipogenesis by regulating miR-140 (Gernapudi et al., 2016). ANCR is an adipocyte differentiation-associated lncRNA that inhibits adipocyte differentiation of ADSCs by competing with miR-204 and augmenting the expression of miR-204 target gene SIRT1 (Li et al., 2016). In contrast, down-regulation of ANCR promotes osteogenic differentiation of periodontal ligament stem cells by regulating the Wnt signaling pathway (Jia, Jiang, & Ni, 2015). The lncRNA H19, one of the most well-known imprinted genes, has recently been shown to enhance osteogenesis through direct activation of the Wnt/β-catenin pathway by functioning as a ceRNA (Liang et al., 2016). In our study, we found that lncRNA TCONS_00041960 (located on chromosome 14 from 57325205 to 57325264 and 1,669 bp in length) was down-regulated in glucocorticoid-treated rat BMSCs by lncRNA microarray analysis. Further experiments revealed that up-regulation of TCONS_00041960 decreased expression of adipogenesis-associated genes PPARγ and C/EBPα, and elevated expression of osteogenesis-associated genes Runx2, osterix, and osteocalcin, which were consistent with their protein levels. These data indicated that TCONS_00041960 partially counteracted glucocorticoid-induced adipogenic differentiation of rat BMSCs and promoted osteogenic differentiation.

Based on our data, lncRNAs are indeed involved in adipogenesis and osteogenesis of rat BMSCs. However, the underlying mechanism remains unknown. Thus far, the mechanisms of lncRNA functions have

been roughly classified into the following categories: (1) transcriptional regulation, lncRNAs regulate transcriptional activation or silencing of genes and interact with chromatin modifiers (Akhade, Pal, & Kanduri, 2017); (2) post-transcriptional regulation: lncRNAs participate in splicing, editing, transport, translation, and degradation and even as miRNA sponges in post-transcriptional processing of mRNAs (Yoon, Abdelmohsen, & Gorospe, 2013); (3) other mechanisms: lncRNAs may function by regulating protein localization, telomere replication, and RNA interference other than transcriptional regulation and post-transcriptional regulation (Ma, Bajic, & Zhang, 2013). Among these mechanisms, the functions of a lncRNA sponge or decoy miRNA have received much attention. For example, muscle-specific lncRNA lic-MD1 as a sponge of miR-133 and miR-135 enhances muscle-specific gene expression of MAML1 and MEF2C, respectively (Cesana et al., 2011). Similarly, lncRNA H19 promotes osteoblastic differentiation of human BMSCs by functioning as miR-141 and miR-22 sponges to de-repress their target gene, β-catenin (Liang et al., 2016). Similarly, lncRNA-MODR, an osteogenesis differentiation-related lncRNA of maxillary sinus membrane stem cells, acts as a molecular sponge of miR-454 to prevent miR-454-mediated suppression of Runx2 (Weng, Peng, Zhu, & Chen, 2017). Here, based on bioinformatics prediction and sequence analysis, we found binding sites between TCONS_00041960 and miR-204-5p as well as miR-125a-3p. Therefore, we speculated that TCONS_00041960 may interact with miR-204-5p and miR-125a-3p. Through luciferase reporter assays, we confirmed that TCONS_00041960 recognized the seed regions of miR-204-5p and miR-125a-3p. Furthermore, RIP and SPR assays showed that TCONS_00041960 functioned as a sponge of miR-204-5p and miR-125a-3p, and thus sequesters them from potential mRNAs (An, Furber, & Ji, 2017). We also found that siRNA against TCONS_00041960 increased miR-204-5p and miR-125a-3p expression. However, over-expression of TCONS_00041960 repressed their expression. Considering the reciprocal influence, lncRNAs can be controlled by miRNAs. TreRNA, a cancer progression-related lncRNA, can be suppressed by miR-190a in hepatoma progression (Wang et al., 2015). The stability of LncRNA-p21 decreases by over-expression of miRNA let-7b and RNA-binding proteins HuR and Ago2 (a component of the RNA-induced silencing complex) in human cervical carcinoma (Yoon et al., 2012). Similarly in our study, over-expressed miR-204-5p or miR-125a-3p depleted expression of TCONS_00041960 in BMSCs. Conversely, siRNAs against miR-204-5p or miR-125a-3p elevated expression of TCONS_00041960. These data demonstrated that TCONS_00041960 as a ceRNA interacted with miR-204-5p and miR-125a-3p. The ceRNA hypothesis proposes that lncRNAs as ceRNAs can sponge miRNAs and directly or indirectly affect the stability of target mRNAs (Salmena, Poliseno, Tay, Kats, & Pandolfi, 2011). In accordance with the ceRNA hypothesis, we speculated that TCONS_00041960 influences the targets of miR-204-5p or miR-125a-3p.

Runx2 is one of most important transcription factors necessary for osteogenesis and activation of osteoblast differentiation marker genes, which plays a vital role in bone formation and metabolism (Shahi, Peymani, & Sahmani, 2017). Much is known about Runx2, but not GILZ. GILZ inhibits key adipogenic regulator PPARγ and blocks adipocyte differentiation (Shi et al., 2003). A recent study showed that up-regulated GILZ in BMSCs enhances osteogenesis (He, Yang, Isales, & Shi, 2012) and increases bone acquisition by inhibition of PPARγ gene transcription (Pan et al., 2014). In glucocorticoid-treated BMSCs, expression of adipogenic gene PPARγ was negatively correlated to that of osteogenic gene Runx2. Glucocorticoids significantly induce BMSC differentiation into adipocytes and suppress their differentiation into osteocytes (Yin, Li, & Wang, 2006). In our study, bioinformatics analysis, luciferase reporter assays, and western blotting confirmed that miR-204-5p targets Runx2 and miR-125a-3p targets GILZ. Furthermore, siRNA against miR-204-5p derepressed the inhibition of Runx2 in glucocorticoid-treated BMSCs, and siRNA against miR-125a-3p rescued GILZ expression. These results demonstrated that miR-204-5p and miR-125a-3p target Runx2 and GILZ, respectively, which are involved in adipogenesis and osteogenesis of glucocorticoid-treated BMSCs.

Taken together, our results suggest that TCONS_00041960 functions as a ceRNA by directly sponging miR-204-5p and miR-125a-3p to simultaneously regulate Runx2 and GILZ expression in glucocorticoid-treated BMSCs. We found that TCONS_00041960 participates in regulating adipogenic and osteogenic differentiation of glucocorticoid-treated BMSCs. Further experiments showed that TCONS_00041960 interacts with miR-204-5p and miR-125a-3p to regulate osteogenic marker Runx2 and adipogenic marker GILZ, respectively. Hence, we revealed a new TCONS_00041960-miR-204-5p/miR-125a-3p-Runx2/GILZ axis involved in adipogenesis and osteogenesis of glucocorticoid-treated BMSCs. Additional research may fully elucidate the intricate modulation network of TCONS_00041960 and provide a potential therapeutic target for glucocorticoid-induced ONFH.

ACKNOWLEDGMENTS

The authors are grateful to all staff who contributed to this study. This work was supported by National Natural Science Foundation of China (grant number: 81772427).

CONFLICTS OF INTEREST

All the authors declare that they do not have potential conflicts of interest.

ORCID

Guowei Shang http://orcid.org/0000-0002-0607-4663

REFERENCES

Akhade, V. S., Pal, D., & Kanduri, C. (2017). Long noncoding RNA: Genome organization and mechanism of action. *Advances in Experimental Medicine and Biology*, *1008*, 47–74.

Ambros, V., & Chen, X. (2007). The regulation of genes and genomes by small RNAs. *Development (Cambridge, England)*, *134*(9), 1635–1641.

An, Y., Furber, K. L., & Ji, S. (2017). Pseudogenes regulate parental gene expression via ceRNA network. *Journal of Cellular and Molecular Medicine*, *21*(1), 185–192.

Brosnan, C. A., & Voinnet, O. (2009). The long and the short of noncoding RNAs. *Current Opinion in Cell Biology*, *21*(3), 416–425.

Cesana, M., Cacchiarelli, D., Legnini, I., Santini, T., Sthandier, O., Chinappi, M., … Bozzoni, I. (2011). A long noncoding RNA controls muscle differentiation by functioning as a competing endogenous RNA. *Cell*, *147*(2), 358–369.

Drescher, W., Schlieper, G., Floege, J., & Eitner, F. (2011). Steroid-related osteonecrosis—An update. *Nephrology, Dialysis, Transplantation: Official Publication of the European Dialysis and Transplant Association—European Renal Association*, *26*(9), 2728–2731.

Fatica, A., & Bozzoni, I. (2014). Long non-coding RNAs: New players in cell differentiation and development. *Nature Reviews Genetics*, *15*(1), 7–21.

Gernapudi, R., Wolfson, B., Zhang, Y., Yao, Y., Yang, P., Asahara, H., & Zhou, Q. (2016). MicroRNA 140 promotes expression of long noncoding RNA NEAT1 in adipogenesis. *Molecular and Cellular Biology*, *36*(1), 30–38.

He, L., Yang, N., Isales, C. M., & Shi, X. M. (2012). Glucocorticoid-induced leucine zipper (GILZ) antagonizes TNF-alpha inhibition of mesenchymal stem cell osteogenic differentiation. *PLoS ONE*, *7*(3), e31717.

Ikeuchi, K., Hasegawa, Y., Seki, T., Takegami, Y., Amano, T., & Ishiguro, N. (2015). Epidemiology of nontraumatic osteonecrosis of the femoral head in Japan. *Modern Rheumatology*, *25*(2), 278–281.

Jia, Q., Jiang, W., & Ni, L. (2015). Down-regulated non-coding RNA (lncRNA-ANCR) promotes osteogenic differentiation of periodontal ligament stem cells. *Archives of Oral Biology*, *60*(2), 234–241.

Jones, J. P., Jr. (1993). Fat embolism, intravascular coagulation, and osteonecrosis. *Clinical Orthopaedics and Related Research*, (292), 294–308.

Kitagawa, M., Kitagawa, K., Kotake, Y., Niida, H., & Ohhata, T. (2013). Cell cycle regulation by long non-coding RNAs. *Cellular and Molecular Life Sciences: CMLS*, *70*(24), 4785–4794.

Kung, J. T., Colognori, D., & Lee, J. T. (2013). Long noncoding RNAs: Past, present, and future. *Genetics*, *193*(3), 651–669.

Li, M., Sun, X., Cai, H., Sun, Y., Plath, M., Li, C., … Chen, H. (2016). Long non-coding RNA ADNCR suppresses adipogenic differentiation by targeting miR-204. *Biochimica Et Biophysica Acta*, *1859*(7), 871–882.

Li, Z., Jin, C., Chen, S., Zheng, Y., Huang, Y., Jia, L., … Zhou, Y. (2017). Long non-coding RNA MEG3 inhibits adipogenesis and promotes osteogenesis of human adipose-derived mesenchymal stem cells via miR-140-5p. *Molecular and Cellular Biochemistry*, *433*(1–2), 51–60.

Liang, W. C., Fu, W. M., Wang, Y. B., Sun, Y. X., Xu, L. L., Wong, C. W., … Zhang, J. F. (2016). H19 activates Wnt signaling and promotes osteoblast differentiation by functioning as a competing endogenous RNA. *Scientific Reports*, *6*, 20121.

Lu, L., Sun, K., Chen, X., Zhao, Y., Wang, L., Zhou, L., … Wang, H. (2013). Genome-wide survey by ChIP-seq reveals YY1 regulation of lincRNAs in skeletal myogenesis. *The EMBO Journal*, *32*(19), 2575–2588.

Ma, L., Bajic, V. B., & Zhang, Z. (2013). On the classification of long non-coding RNAs. *RNA Biology*, *10*(6), 925–933.

Mont, M. A., & Hungerford, D. S. (1995). Non-traumatic avascular necrosis of the femoral head. *The Journal of Bone and Joint Surgery American*, *77*(3), 459–474.

Mont, M. A., Jones, L. C., & Hungerford, D. S. (2006). Nontraumatic osteonecrosis of the femoral head: Ten years later. *The Journal of Bone and Joint Surgery American*, *88*(5), 1117–1132.

Pan, G., Cao, J., Yang, N., Ding, K., Fan, C., Xiong, W. C., … Shi, X. M. (2014). Role of glucocorticoid-induced leucine zipper (GILZ) in bone acquisition. *The Journal of Biological Chemistry*, *289*(28), 19373–19382.

Pasquinelli, A. E. (2012). MicroRNAs and their targets: Recognition, regulation and an emerging reciprocal relationship. *Nature Reviews Genetics*, *13*(4), 271–282.

Salmena, L., Poliseno, L., Tay, Y., Kats, L., & Pandolfi, P. P. (2011). A ceRNA hypothesis: The Rosetta Stone of a hidden RNA language? *Cell*, *146*(3), 353–358.

Shahi, M., Peymani, A., & Sahmani, M. (2017). Regulation of bone metabolism. *Reports of Biochemistry & Molecular Biology*, *5*(2), 73–82.

Shi, X., Shi, W., Li, Q., Song, B., Wan, M., Bai, S., & Cao, X. (2003). A glucocorticoid-induced leucine-zipper protein, GILZ, inhibits adipogenesis of mesenchymal cells. *EMBO Reports*, *4*(4), 374–380.

Tan, G., Kang, P. D., & Pei, F. X. (2012). Glucocorticoids affect the metabolism of bone marrow stromal cells and lead to osteonecrosis of the femoral head: A review. *Chinese Medical Journal*, *125*(1), 134–139.

Tye, C. E., Gordon, J. A., Martin-Buley, L. A., Stein, J. L., Lian, J. B., & Stein, G. S. (2015). Could lncRNAs be the missing links in control of mesenchymal stem cell differentiation? *Journal of Cellular Physiology*, *230*(3), 526–534.

Wang, Q., Li, Y., Zhang, Y., Ma, L., Lin, L., Meng, J., … Zhang, Y. (2017). LncRNA MEG3 inhibited osteogenic differentiation of bone marrow mesenchymal stem cells from postmenopausal osteoporosis by targeting miR-133a-3p. *Biomedicine & Pharmacotherapy=Biomedecine & Pharmacotherapie*, *89*, 1178–1186.

Wang, X., Ren, Y., Yang, X., Xiong, X., Han, S., Ge, Y., … Yang, M. (2015). MiR-190a inhibits epithelial-mesenchymal transition of hepatoma cells via targeting the long non-coding RNA treRNA. *FEBS Letters*, *589*(24 Pt B), 4079–4087.

Weinstein, R. S. (2012). Glucocorticoid-induced osteonecrosis. *Endocrine*, *41*(2), 183–190.

Weng, J., Peng, W., Zhu, S., & Chen, S. (2017). Long noncoding RNA sponges miR-454 to promote osteogenic differentiation in maxillary sinus membrane stem cells. *Implant Dentistry*, *26*(2), 178–186.

Yin, L., Li, Y. B., & Wang, Y. S. (2006). Dexamethasone-induced adipogenesis in primary marrow stromal cell cultures: Mechanism of steroid-induced osteonecrosis. *Chinese Medical Journal*, *119*(7), 581–588.

Yoon, J. H., Abdelmohsen, K., & Gorospe, M. (2013). Posttranscriptional gene regulation by long noncoding RNA. *Journal of Molecular Biology*, *425*(19), 3723–3730.

Yoon, J. H., Abdelmohsen, K., Srikantan, S., Yang, X., Martindale, J. L., De, S., … Gorospe, M. (2012). LincRNA-p21 suppresses target mRNA translation. *Molecular Cell*, *47*(4), 648–655.

Zhang, K., Huang, K., Luo, Y., & Li, S. (2014). Identification and functional analysis of long non-coding RNAs in mouse cleavage stage embryonic development based on single cell transcriptome data. *BMC Genomics*, *15*, 845.

Zhao, D. W., Yu, M., Hu, K., Wang, W., Yang, L., Wang, B. J., … Ma, L. (2015). Prevalence of nontraumatic osteonecrosis of the femoral head and its associated risk factors in the chinese population: Results from a nationally representative survey. *Chinese Medical Journal*, *128*(21), 2843–2850.

Zhao, F. C., Guo, K. J., & Li, Z. R. (2013). Osteonecrosis of the femoral head in SARS patients: Seven years later. *European Journal of Orthopaedic Surgery & Traumatology: Orthopedie Traumatologie*, *23*(6), 671–677.

How to cite this article: Shang G, Wang Y, Xu Y, et al. Long non-coding RNA TCONS_00041960 enhances osteogenesis and inhibits adipogenesis of rat bone marrow mesenchymal stem cell by targeting miR-204-5p and miR-125a-3p. *J Cell Physiol.* 2018;233:6041–6051. https://doi.org/10.1002/jcp.26424